Bridging *versus* Hydride Shift in Gaseous Cations: Hydroxy as a Vicinal Substituent

Viet Nguyen, Jacqueline S. Bennett, and Thomas Hellman Morton*

Contribution from the Department of Chemistry, University of California, Riverside, California 92521-0403

Received June 17, 1996. Revised Manuscript Received February 15, 1997[⊗]

Abstract: Primary cations of the form $XCH_2CH_2^+$ (**1**) are unstable with respect to the bridged isomer cyclo-$(CH_2)_2X^+$ (**2**) or the hydride-shift isomer CH_3CHX^+ (**3**). Two independent hydrogen isotope experiments for $X = OH$ demonstrate that gaseous $HOCH_2CH_2^+$ (**1a**) gives less of its bridged isomer, protonated oxirane (**2a**), than of its hydride-shift isomer, protonated acetaldehyde (**3a**). Metastable ion decompositions of ionized $HOCH_2CH_2OPh$ show that the radical cation decomposes via an ion–neutral complex containing **3a** and phenoxy radical. Deuterium labeling studies exhibit no detectable interconversion of the two sp^3-carbons, implying that complexes containing **2a** are not formed to a measurable extent. An independent neutral product study looks at the radioactive oxirane and acetaldehyde produced when tritium on the methyl group of gaseous $CH_2TCHTOH$ undergoes radioactive decay. Loss of a beta-particle and a helium atom forms transient, tritiated **1a**. Ions from isomerization of this radiolabeled primary cation were deprotonated by Me_3N and gave a >97% yield of acetaldehyde. Quantitative assessment of possible routes to acetaldehyde (including rearrangement of excited **2a**) implies that **1** undergoes hydride shift at least 5 times faster than bridging by neighboring oxygen.

Nonconjugated primary carbocations are notoriously labile and rearrange rapidly to more stable isomers. For β-substituted ethyl cations (**1**) two rearrangement pathways compete with one another: neighboring group participation via bridging (i) versus hydride shift (ii). These pathways tend to operate in concert
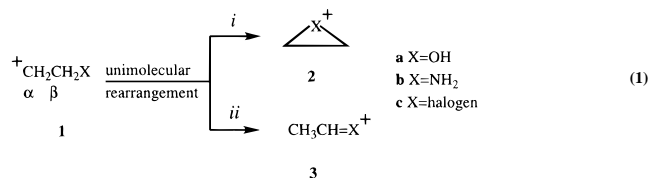
with bond heterolysis when solvolysis produces cations with the nominal structure **1**. In solution, bridging predominates when X is an amino group[1] or a halogen (Cl, Br, or I),[2] but it is not easy to form **1** (even nominally) when $X = OR$[3] (although more highly substituted carbon skeletons are known to exhibit oxygen bridging[1]). In the gas phase, bridging to form **2b** or **2c** has been reported when radical cations heterolyze to yield **1** in cases where $X = NH_2$[4] or F.[5,6] Competition between bridging and hydride transfer is known for neighboring OH in reactions of higher homologues, such as loss of neutral YH from CH_3-$CH(OH)CH(YH^+)CH_3$ ions in the gas phase,[7] but the simplest system **1** (or its nominal equivalents) is less well documented for $X = OH$. Bridged ions (**2**) containing oxygen have higher heats of formation than their acyclic isomers (**3**). Gaseous,

protonated acetaldehyde (**3a**) is $\Delta H_{3a \rightarrow 2a} = 110$ kJ mol^{-1} (26 kcal mol^{-1}) more stable than protonated oxirane (**2a**).[8] This is close to the value for $X = NH_2$, $\Delta H_{3b \rightarrow 2b} \approx 100$ kJ mol^{-1},[8,9] where kinetic control favors **2b**. For $X =$ halogen, thermodynamic control should also favor pathway ii unless the bridging atom is bromine or larger.[10]

Bridging tends to reflect intramolecular S_N2-type chemistry, as shown by stereochemical experiments on gaseous 2,3-disubstituted butanes.[7] Epoxides form rapidly in solution from YCH_2CH_2X via loss of leaving group Y when $X = O^-$, because the anionic nucleophile rapidly effects backside displacement. Internal S_N2 also takes place when X is an amine. This paper compares rearrangement of "free" gaseous **1** with gas-phase C–Y bond heterolysis in $XCH_2CH_2Y^+$ ions. The outcome is not what might have been expected on the basis of higher homologues.

The most reliable published ab initio calculations suggest that β-hydroxyethyl cation (**1a**) does not correspond to a stable geometry.[11] Ion **1a** should have, at best, a fleeting existence, even when rigorously isolated from other molecules. Two experimental techniques are available for probing gaseous primary cations of this nature. Under one set of experimental conditions, **1a** nominally intervenes during C–Y heterolysis of a $HOCH_2CH_2Y^+$ precursor, in which eq 1 probably operates in concert with the bond fission. The other experiment examines "free" **1a** created on the time scale of a single molecular vibration. In either case we find that the favored rearrangement occurs via pathway ii.

[⊗] Abstract published in *Advance ACS Abstracts,* August 15, 1997.

(1) Streitwieser, A., Jr. *Solvolytic Displacement Reactions*; McGraw-Hill: New York, 1962.

(2) Olah, G. A. *Halonium Ions*; Wiley-Interscience: New York, 1975.

(3) Olah, G. A.; White, A. M.; O'Brien, D. H. In *Carbonium Ions*, Olah, G. A., Schleyer, P. v. R., Eds.; Wiley-Interscience: New York, 1973; Vol. IV, pp 1697–1781.

(4) Van de Sande, C. C.; Ahmad, S. Z.; Borchers, F.; Levsen, K. *Org. Mass Spectrom.* **1978**, *13*, 666–670.

(5) Ciommer, B.; Schwarz, H. *Z. Naturforsch.* **1983**, *38B*, 635–638.

(6) Nguyen, V.; Cheng, X.; Morton, T. H. *J. Am. Chem. Soc.* **1992**, *114*, 7127–7132.

(7) Angelini, G.; Speranza, M. *J. Am. Chem. Soc.* **1981**, *103*, 3800–3806.

(8) Lias, S. G.; Liebman, J. F.; Holmes, J. L.; Levin, R. D.; Mallard, W. G. *J. Phys. Chem. Ref. Data* **1988**, *17*, Suppl 1.

(9) Lossing, F. P.; Lam, Y.-T.; Maccoll, A *Can. J. Chem.* **1981**, *59*, 2228–2231.

(10) Reynolds, C. H. *J. Am. Chem. Soc.* **1992**, *114*, 8676–8682.

(11) For $X = OH$ (**1a**) SCF calculations using the 6-31G* basis set have been reported, which predict a stable classical β-hydroxyethyl cation (Benassi, R.; Taddei, F. *J. Mol. Struct.* **1990**, *205*, 177–190). Higher level computations, however, exhibit a negative force constant (Bock, C. W.; George, P.; Glusker, J. P. *J. Org. Chem.* **1993**, *58*, 5816–5825). These latter authors calculate a 1.2 eV energy barrier (MP2/6-31G*//MP2/6-31G*) for isomerization of **2a** to **3a**.

Experimental Section

Mass-Resolved Ion Kinetic Energy Spectra (MIKES). Mass spectrometric experiments were performed on VG ZAB-2F and VG ZAB-2SE (B-E) double-focusing instruments with 70 eV electron ionization. Commercial 2-phenoxyethanol (**4**) was used without further purification, while **4**-α,α-d_2, **4**-β,β-d_2, $C_6D_5OCH_2CH_2OH$ (**4-d_5**), and $PhOCD_2COOH$ were prepared (>98 atom % D) as previously described.[6] 1,1,2,2-Tetradeuterio-2-phenoxyethanol (**4**-α,α,β,β-d_4 >98 atom % D) was prepared by $LiAlD_4$ reduction of $PhOCD_2COOH$. O-deuterated phenoxyethanols were prepared by exchange with D_2O in the ZAB source.

Neutral Products from [3]H Decay. Ditritiated ethanol **9** was freshly prepared by transesterification of tritiated ethyl docosanoate (specific activity ~0.05 Ci μmol^{-1} from catalytic reduction of vinyl docosanoate with tritium gas, performed at the National Tritium Labeling Facility) with docosanol. This tritiated ester had been purified by preparative HPLC a few weeks before conversion to **9**. The transesterification was catalyzed by titanium tetradocosoxide and performed in a sealed glass apparatus under vacuum. Vapor of the radiolabeled ethanol product was condensed in a liquid nitrogen-cooled bulb containing frozen NMe_3 and the apparatus sealed and allowed to come to room temperature, where its contents were entirely gaseous. Thus, a 0.02 Ci sample of gaseous tritiated ethanol was sealed in a 1 L Pyrex bulb with 0.5 atm of NMe_3 and allowed to stand in the dark at room temperature for 11 months (2.9×10^7 s = 0.075 half-lives). In this interval 5% of the tritium nuclei decay. The gaseous reaction mixture was then condensed at liquid nitrogen temperature, and a large excess of unlabeled oxirane was vacuum transferred into the bulb and mixed with the condensate. A portion was transferred to a sealed tube and reacted with phenol (containing 8 mol % sodium phenoxide) to give $PhOCH_2CH_2OH$, which was converted to its *N*-phenylcarbamate ester, recrystallized 3 times from ethanol and once from CCl_4, and radioassayed by liquid scintillation counting. From the specific activity of tritium in this solid derivative we infer the yield of tritiated oxirane to have been ≤0.02 mCi. The remainder of the sample was diluted with a large excess of unlabeled acetaldehyde in ethanol solution, converted to the semicarbazone, recrystallized three times from ethanol, and radioassayed by liquid scintillation counting. From the specific activity of tritium in that solid derivative we infer the yield of tritiated acetaldehyde to have been 0.9 ± 0.1 mCi.

Theoretical Calculations. Ab initio SCF calculations were performed by means of SPARTAN (Wavefunction, Inc.) and GAUSSIAN 94 (Gaussian, Inc.), with geometries optimized using Hartree−Fock (HF) based methods and the 6-31G** basis set. The basis set superposition error (BSSE) was estimated using the counterpoise method, and SCF zero-point energy differences at 6-31G** are scaled by a factor of 0.89 in determining calculated values of Δ*H*. To minimize spin contamination, single-point density functional calculations were performed on the HF-optimized geometries at B3LYP using the same basis set.

Results

Gas-phase techniques provide avenues to nascent primary cations, which are difficult to access in solution. One approach makes use of ionic decompositions in the mass spectrometer that have been described as gas-phase analogues of solvolysis.[12,13] As in conventional solvolyses, rearranged ions are formed in association with a noncovalently bound partner. In the gas phase this partner is neutral, but the overall behavior is analogous to formation of an ion pair in solution. In the present study mass spectrometric decompositions of ionized $PhOCH_2$-CH_2OH implicate a $[C_2H_5O^+ \ PhO^\bullet]$ complex, whose subsequent chemistry is interpreted with the aid of the SCF calculations summarized in Table 1. As discussed below, positions α and β do not interconvert in the majority of ions. This rules out pathway i as the dominant rearrangement.

(12) McAdoo, D. G.; Morton, T. H. *Acc. Chem. Res.* **1993**, *26*, 295−302.

(13) (a) Morton, T. H. *J. Am. Chem. Soc.* **1980**, *102*, 1596−1602. (b) Morton, T. H. *Tetrahedron* **1982**, *38*, 3195−3243.

Table 1. Local Minima on the $C_8H_{10}O_2$ and $C_8H_{10}O_2^{\bullet+}$ 6-31G** Potential Energy surfaces: E^{rel} for UHF-Optimized Structures (kJ mol^{-1}) (to the nearest 0.5) Relative to Ionized Phenol plus Neutral Acetaldehyde, Including Zero-Point and Counterpoise Corrections, and Differences between HF and Density Functional (DFT)^c Electronic Energies (au)

	E^{elec}_{HF} (au)	E^{rel}_{UHF}	$\langle S^2 \rangle_{HF}{}^b$	$E^{elec}_{HF} - E^{elec}_{DFT}$	$\langle S^2 \rangle_{DFT}{}^b$
4a (*anti*)	−458.491 327		0	2.816 611	0
4b (*gauche*)	−458.488 129		0	2.817 435	0
4c (H−bond)	−458.493 850		0	2.818 299	0
CH_3CHO	−152.922 587		0	0.911 796	0
PhOH$^{\bullet+}$	−305.320 581^a		0.7984	1.861 051	0.7658
4a$^{\bullet+}$	−458.248 720^a	17	1.0685	2.775 00	0.7661
4b$^{\bullet+}$	−458.255 381^a	−0.5	1.0814	2.776 030	0.7677
5	−458.201 850^a	137.5	0.7501	2.784 929	0.7531
7	−458.281 391^a	−91.5	1.0862	2.776 464	0.7678
8	−458.237 055^a	24.5	0.7598	2.778 377	0.7521
9	−458.244 757^a	4.5	0.7599	2.776 251	0.7521

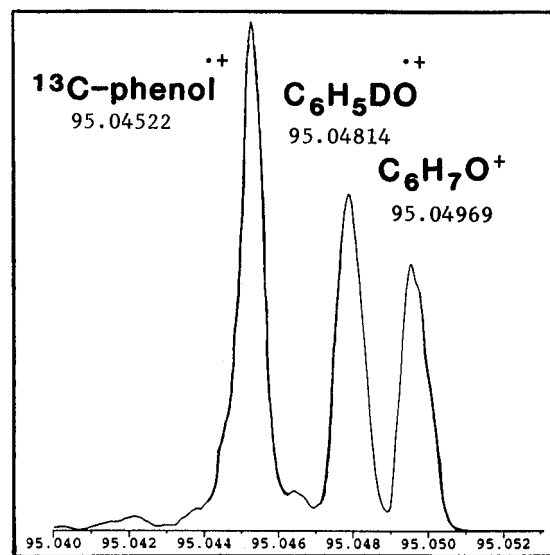^{a} UHF-optimized. ^{b} Before annihilation. ^{c} B3YLP/6-31G**//UHF/6-31G** single-point calculation.

Figure 1. Double-focusing source mass spectrum (7×10^4 resolution) of *m/z* 95 from 70 eV electron ionization of $PhOCH_2CD_2OH$.

The mass spectrum of $PhOCH_2CD_2OH$ illustrates pertinent issues. Under ordinary electron ionization conditions *m/z* 94 (phenol$^{\bullet+}$) represents the base peak. The neighboring ion at *m/z* 95 consists of three components, as the high-resolution mass spectrum in Figure 1 reveals. The largest corresponds to natural abundance [^{13}C]phenol$^{\bullet+}$, whose intensity (relative to the intensity of *m/z* 94 as 100) should be 6.6. The other two peaks correspond to $C_6H_5DO^{\bullet+}$ and protonated phenol ($C_6H_7O^+$), with relative intensities of 4.6 and 3.5, respectively. The deuterated ion results from a small amount of hydrogen transposition between the chain and the ring, as further implied by the 70 eV GC/MS of $C_6D_5CH_2CH_2OH$, in which $C_6HD_5O^{\bullet+}$ (*m/z* 99) contributes the base peak, *m/z* 98 has a relative intensity of 6.5, and protonated phenol-d_5 (*m/z* 100) has a relative intensity of 5 (after subtraction of the natural abundance ^{13}C contibution). Chain/ring exchange has previously been noted by Nibbering and co-workers in ionized $PhOCH_2CH_2F$.[14] The intervention of ion−neutral complexes can account for it in the present case, as will be discussed below.

(14) (a) Theissling, C. B.; Nibbering, N. M. M. *Adv. Mass Spectrom.* **1978**, *7b*, 1287−1295. (b) Borchers, F.; Levsen, K.; Nibbering, N. M. M.; Theissling, C. B. *Org. Mass Spectrom.* **1977**, *12*, 746−750. (c) Russell, D. H.; Gross, M. L.; van der Greef, J.; Nibbering, N. M. M. *Org. Mass Spectrom.* **1979**, *14*, 474−479.
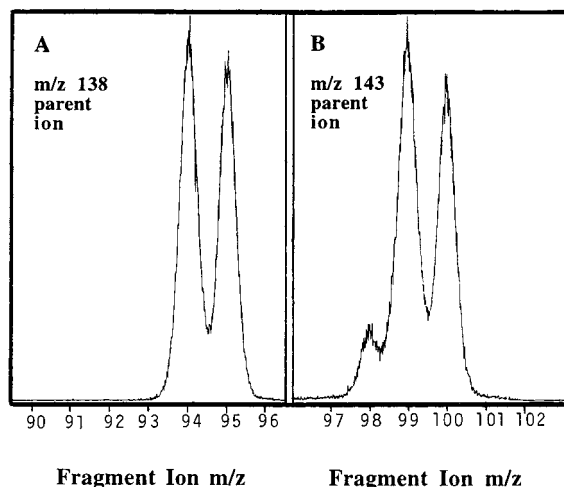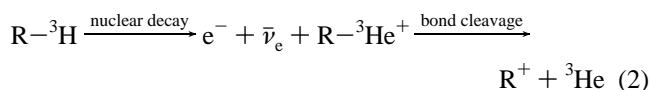
Figure 2. Mass-resolved ion kinetic energy spectra (MIKES) of metastable ionized 2-phenoxyethanol (C$_6$H$_5$OCH$_2$CH$_2$OH; A) and its ring-deuterated analogue **4**-d_5 (C$_6$D$_5$OCH$_2$CH$_2$OH; B).

The formation of protonated phenol provides a subject worthy of closer scrutiny. Net transfer of two hydrogens from the $-$CH$_2$CH$_2$OH group offers a way to detect interconversion of positions α and β. The presence of C$_6$H$_7$O$^+$ in Figure 1 shows that hydrogen transposition occurs at detectable levels in the 70 eV source mass spectrum. At the lower internal energies that typify metastable ion decompositions, though, α,β-interconversion contributes far less than it does in the source. Metastable PhOCH$_2$CH$_2$OH$^{\bullet+}$ decomposes in the second field-free region of our mass spectrometer to give a proportion of protonated phenol ion nearly equal to the yield of phenol$^{\bullet+}$, but with no evidence at all of oxygen bridging. The results detailed below focus upon metastable ion decompositions as a way to probe nascent **1a**.

An alternative approach makes use of nuclear decay of tritium, eq 2, to yield free gaseous cations.[15] The Discussion

$$\text{R}-^3\text{H} \xrightarrow{\text{nuclear decay}} e^- + \bar{\nu}_e + \text{R}-^3\text{He}^+ \xrightarrow{\text{bond cleavage}}$$
$$\text{R}^+ + {}^3\text{He} \quad (2)$$

presents arguments to sustain the view that R$^+$ initially formed as **1** in this fashion will rearrange, and a substantial fraction will retain structures **2** or **3** long enough to be quenched by gaseous base. If the radiolabeled, neutral precursor contains >1 tritium, R$^+$ will be radiolabeled, too. Uncharged radioactive products recovered from its neutralization will reflect the structure of R$^+$. Experimental data from the two approaches are given below.

Metastable Ion Decompositions of Ionized 2-Phenoxyethanol. Results from mass spectrometry will be presented first. Metastable ionized PhOCH$_2$CH$_2$OH (**4**$^{\bullet+}$) exhibits two fragment ions in the mass-resolved ion kinetic energy spectrum (MIKES): ionized phenol (m/z 94) and protonated phenol (m/z 95) in the ratio C$_6$H$_6$O$^{\bullet+}$:C$_6$H$_7$O$^+$ = 1.2:1. Spectrum A in Figure 2 reproduces these fragment peaks. Since MIKES cannot achieve the resolution shown in Figure 1, we evaluate the extent of chain/ring hydrogen transposition using **4**-d_5. When the phenyl group is perdeuterated, the d_5 molecular ion (**4**$^{\bullet+}$-d_5) exhibits three fragment ions, m/z 98, 99, and 100, in the ratio C$_6$H$_2$D$_4$O$^{\bullet+}$:C$_6$HD$_5$O$^{\bullet+}$:C$_6$D$_5$O$^+$ = 0.2:1.3:1, as spectrum B in Figure 2 depicts. The intensity of m/z 97 is $\leq$ 1/20 the intensity of m/z

(15) Cacace, F.; Speranza, M. In *Techniques for the Study of Ion-Molecule Reactions*; Farrar, J. M., Saunders, W. H., Jr., Eds.; Techniques of Chemistry XX; Wiley-Interscience: New York, 1988; pp 287−323.

Table 2. Abundances of Fragment Ions in 70 eV MIKES Spectra of Ionized 2-Phenoxyethanol (**1**$^{\bullet+}$) and Its Chain-Deuterated Analogues Relative to the Intensity (=1.0) of the Highest Mass Ion

parent neutral	m/z 94	m/z 95	m/z 96	m/z 97
C$_6$H$_5$OCH$_2$CH$_2$OH	1.2	1.0	0.0	0.0
C$_6$H$_5$OCH$_2$CH$_2$OD	0.0	1.2	1.0	0.0
C$_6$H$_5$OCH$_2$CD$_2$OH	0.84	0.48	1.0	0.0
C$_6$H$_5$OCH$_2$CD$_2$OD	0.0	0.94	0.38	1.0
C$_6$H$_5$OCD$_2$CH$_2$OH	1.3	1.0	0.0	0.0
C$_6$H$_5$OCD$_2$CH$_2$OD	0.0	1.3	1.0	0.0
C$_6$H$_5$OCD$_2$CD$_2$OH	0.84	0.42	1.0	0.0
C$_6$H$_5$OCD$_2$CD$_2$OD	0.0	0.93	0.39	1.0

98. The m/z 98:m/z 99 ratio has slightly more than twice the value measured in the source mass spectrum.

The MIKES shows hydrogen exchange within **4**$^{\bullet+}$-d_5 to a greater extent than observed in Figure 1. One possible interpretation of the C$_6$H$_2$D$_4$O$^{\bullet+}$ fragment hypothesizes a chain-ring exchange via a distonic ion intermediate, such as **5**-d_5, which would result from transposition of hydrogen from the carbinol methylene to an *ortho*-position of the benzene ring. In order for the observed mixture of C$_6$H$_2$D$_4$O$^{\bullet+}$ and C$_6$HD$_5$O$^{\bullet+}$ to obtain, this transposition must be reversible, as eq 3 portrays.
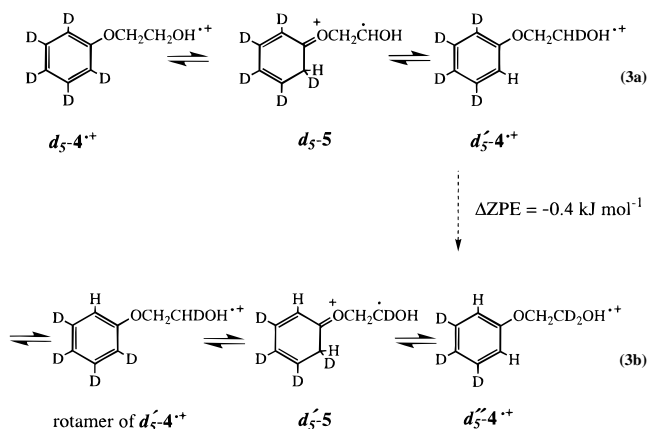

This would lead to an isomerized molecular ion, **4**$^{\bullet+}$-d'_5, whose dissociation should produce ionized phenol-d_4. Our SCF calculations, however, suggest that this interconversion could not be proceeding to equilibrium in the mass spectrometer, since the zero-point energy difference (ΔZPE) between **4**$^{\bullet+}$-d_5 and **4**$^{\bullet+}$-d'_5 favors the latter by 0.3 kJ mol^{-1}.

If the exchange were to operate as represented by eq 3a, however, it should proceed further, via distonic ion **5**-d'_5 and the isomerized molecular ion **4**$^{\bullet+}$-d''_5, as eq 3b depicts. The SCF electronic energy barrier to rotation about the sp^2 C$-$O bond is 58 kJ mol^{-1}, considerably less than the calculated energetic difference between **4**$^{\bullet+}$ and its distonic isomer **5**, 138 kJ mol^{-1} (which includes the BSSE difference and a ΔZPE = -4 kJ mol^{-1}). Since the ionized phenol fragment from eq 3a (C$_6$H$_2$D$_4$O$^{\bullet+}$) constitutes 15% of the unexchanged PhOH$^{\bullet+}$ (C$_6$HD$_5$O$^{\bullet+}$), simple first-order kinetics imply that eq 3b should afford C$_6$H$_3$D$_3$O$^{\bullet+}$ with an abundance of about 15% C$_6$H$_2$D$_4$O$^{\bullet+}$. The fact that C$_6$H$_3$D$_3$O$^{\bullet+}$ (m/z 97) is not observed argues against eq 3 (or any *ortho*-exchange via distonic intermediates). Since the SCF zero point-energy of **4**$^{\bullet+}$-d''_5 is lower than that of **4**$^{\bullet+}$-d'_5 (as indicated by the dashed arrow in eq 3), it is hard to imagine an isotope effect that would permit eq 3a yet militate against eq 3b at the same time. Hence, the simple argument based on first-order kinetics appears conclusive.

When the OH is replaced by OD in the parent ion, the fragment ion m/z values shift 1 mass unit higher, but their relative proportions remain the same. Table 2 summarizes

Scheme 1
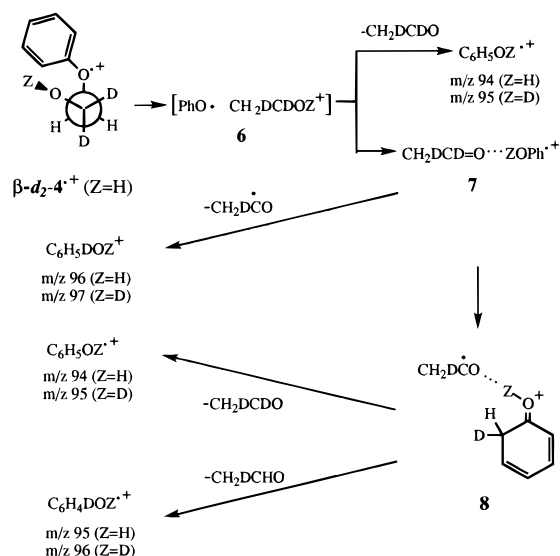
results for all the permutations of deuterium in the chain (perdeuterated methylene groups and the hydroxylic position). Fragment ion ratios are not greatly affected by replacement of OH by OD (although all of the fragment ion masses shift 1 mass unit higher). Scheme 1 outlines a mechanism to account for these results. Hydride shift leads to an ion−neutral complex between phenoxy radical and protonated acetaldehyde, **6**. Either complex decomposes via transfer of hydron Z to yield ionized phenol via loss of acetaldehyde, or it isomerizes to a hydrogen-bonded complex of acetaldehyde with ionized phenol, **7**. Intermediate **7** subsequently decomposes via atom abstraction to yield the conjugate acid of phenol (with concomitant expulsion of acetyl radical), or it isomerizes to a hydrogen-bonded complex between ring-protonated phenol and acetyl radical, such as **8**.

Ionized PhOCD$_2$CH$_2$OD and PhOCH$_2$CD$_2$OD give markedly different fragmentation patterns. The virtual absence of C$_6$H$_5$D$_2$O$^+$ (the intensity of *m/z* 97 is ≤0.04 the intensity of *m/z* 96) in the MIKES of ionized PhOCD$_2$CH$_2$OD (as contrasted with the presence of both *m/z* 96 and *m/z* 97 in the MIKES of PhOCH$_2$CD$_2$OD and PhOCD$_2$CD$_2$OD) implies that positions α and β do not interconvert to a measurable extent within the 10^{-5} s interval prior to the metastable decomposition. The Discussion presents a more detailed analysis of Scheme 1.
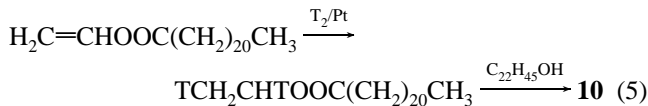
Neutral Product Studies. Free gaseous cations can be produced by beta-decay (expulsion of an electron from within an atomic nucleus) of neutral tritiated molecules. If the neutral precursor contains more than one tritium, its decay product will also be radiolabeled. In the present study, ditritiated ethanol **10** was allowed to decay in the gas phase in the presence of 0.5 atm of trimethylamine (NMe$_3$). The amine served to deprotonate the ion within 10^{-10} s of its formation (assuming an ion−molecule collision rate corresponding to the ADO limit and unit efficiency for proton transfer). The recovered tritium-containing neutral products reflect the structures of the cations produced via eq 4 before they have time to form clusters or to strike the walls of the reaction vessel.

Equation 4 summarizes the anticipated ion structures. Decay of tritium geminal to the OH should produce the conjugate acid ion of tritiated acetaldehyde. Decay of tritium in the methyl group (vicinal to the OH) initially forms tritiated **1a**, whose rearrangement via neighboring group participation (pathway i) should yield the conjugate acid ion of tritiated oxirane. The competing rearrangement of tritiated **1a** via hydride shift
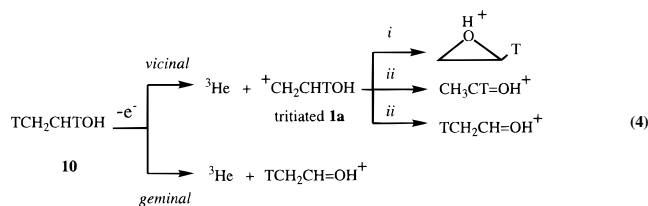
(pathway ii) should yield conjugate acid ions of tritiated acetaldehyde. Deprotonation of these ions in the gas phase by NMe$_3$ affords a mixture of radiolabeled acetaldehyde and radiolabeled oxirane.[16]

The starting point for our synthesis of tritiated ethanol was vinyl docosanoate, which was converted to radiolabeled ethyl docosanoate via catalytic reduction with tritium gas, as eq 5

$$H_2C{=}CHOOC(CH_2)_{20}CH_3 \xrightarrow{T_2/Pt}$$
$$TCH_2CHTOOC(CH_2)_{20}CH_3 \xrightarrow{C_{22}H_{45}OH} \mathbf{10} \quad (5)$$

summarizes. As is well known, catalytic tritiation of double bonds gives a mixture of isomeric products.[17] Hence, the tritiated ethanol in this experiment contains other isotopomers besides **10** (though none of the label is attached to oxygen), including multiply and monotritiated ethyl groups.

^{3}H NMR indicates that some of the tritium resides in monotritiated ethyl groups, but **10** is the predominant labeling pattern. The presence of a variety of tritiated reactants does not vitiate the expected outcome (except that decay of mono-tritiated ethanol will produce unlabeled products, which are not detectable by radioassay). The experiment described here examined the products from 0.02 Ci of tritiated ethanol after decay of 5% of the tritium nuclei. Therefore, labeled ethanol containing, on average, *n* tritia should yield approximately *n* − 1 mCi of tritiated decay products.

Quantitation of the yields of tritiated oxirane and tritiated acetaldehyde provides a measure of the relative proportions of pathways i and ii. The recovered yield of tritiated acetaldehyde was 0.9 ± 0.1 mCi, within experimental uncertainty of the predicted yield of all decay products. The experimentally measured ratio of tritiated acetaldehyde to tritiated oxirane is ≥40:1.

Discussion

The studies reported here embrace theoretical and experimental investigations of the rearrangements of ionic precursors to gaseous β-hydroxyethyl cation, **1a**. Two experimental approaches point to the same conclusion: oxygen bridging is not observed to any great extent. Mass spectrometry of 2-phenoxyethanol provides a set of conditions analogous to solvolysis. Here the primary cation very likely rearranges as it forms, and **1a** represents only a nominal intermediate en route to ion−neutral complexes containing protonated acetaldehyde. A survey of local minima along the ab initio potential energy surface indicates the route followed by metastable ion decompositions. By contrast, theory suggests that nuclear decay offers an approach to a free ion.

Noncovalent Intermediates from Bond Heterolysis of Ionized 2-Phenoxyethanol. C−O bond heterolysis in XCH$_2$-CH$_2$OPh$^{•+}$ produces free C$_2$H$_4$X$^+$ ions (to which cyclic structure **2b** is assigned[4]) when the neighboring group X is NH$_2$. For

(16) Aue, D. H.; Webb, H. M.; Davidson, W. R.; Vidal, M.; Bowers, M. T.; Goldwhite, H.; Vertal, L. E.; Douglas, J. E.; Kollman, P. A.; Kenyon, G. L. *J. Am. Chem. Soc.* **1980**, *102*, 5151−5157.

(17) Williams, P. G.; Morimoto, H.; Wemmer, D. E. *J. Am. Chem. Soc.* **1988**, *110*, 8038−8044.

less basic neighboring groups the heterolysis tends to produce ion−neutral complexes instead. Results from the metastable ion mass spectra of seven deuterated analogues for X = hydroxy can be summarized as follows. (A) Hydrogen transfers exclusively from the OH-group to yield ionized phenol (an odd-electron fragment ion).

(B) One and only one hydrogen from carbon 1 (the CH_2OH) undergoes partial exchange with the benzene ring prior to formation of ionized phenol, while the hydrogens on carbon 2 undergo no such exchange.

(C) Double hydrogen transfer from the chain to yield the conjugate acid of phenol (an even-electron fragment ion) constitutes about 40% of the metastable ion fragment ion current, with one hydrogen coming from the OH group and the other from carbon 1.

Distonic intermediates, exemplified by eq 3, cannot account for the data, as the Results outlines. Limiting the chain-ring hydrogen exchange to one and only one hydrogen requires a mechanism such as depicted in Scheme 1. Before treating this scheme in detail, a summary of SCF calculations on neutral **4** will illustrate consequences of removing an electron. 2-Phenoxyethanol (**4**) has three low-lying conformations, two *gauche* (with respect to the C−C sp^3−sp^3 bond) and one *anti*. The *anti* rotamer, **4a**, is fully extended, with all atoms coplanar (except for the methylene hydrogens) and a mirror plane of symmetry. The less favored *gauche* conformation has no hydrogen bond, and its electronic energy is 8.5 kJ mol^{-1} above that of the *anti* conformation. This *gauche* conformer, **4b**, has a CCOH dihedral angle of 163°, an sp^3 CCOC dihedral angle of 119°, and an OCCO dihedral angle of −73°. The more favored *gauche* conformer, **4c**, has an internal hydrogen bond and dihedral angles similar to those of 2-haloethanols,[18] and its calculated electronic energy is 6.6 kJ mol^{-1} lower than that of the planar *anti*-**4a**. The favored conformation of ionized 2-phenoxyethanol (**4b•+**) has a structure similar to the higher lying *gauche* neutral: dihedral angles CCOH of 179°, sp^3 CCOC of 91°, and OCCO of −64.5°. A Newman projection of the radical cation is drawn schematically in Scheme 1 for **4•+**-β,β-d_2. Even though neutral, hydrogen-bonded **4c** lies 15 kJ mol^{-1} lower in energy than the other *gauche* conformer, **4b**, the radical cation corresponding to the hydrogen-bonded geometry (**4c•+**) is not stable and transforms without a barrier to the more stable molecular ion structure **4b•+**. *anti*-Planar ionized 2-phenoxyethanol (**4a•+**) has an electronic energy 17.5 kJ mol^{-1} higher than that of the favored *gauche* conformer (both have virtually the same BSSE correction).

Equation 6 summarizes potential energy minima that we believe intervene in the decomposition of **4•+** (with UHF/6-31G** $\Delta H°$ values at 0 K). The hydrogen-bonded aggregate
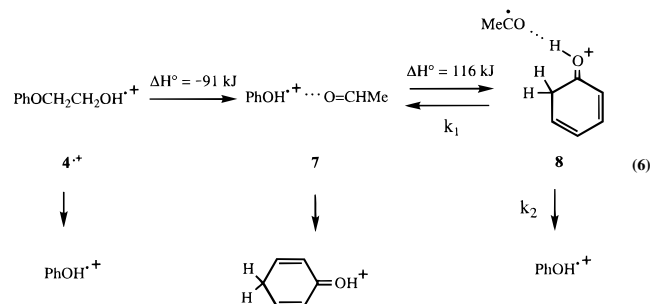
of acetaldehyde with ionized phenol, **7**, is much more stable than **4•+** (the calculated exothermicity for the first step includes
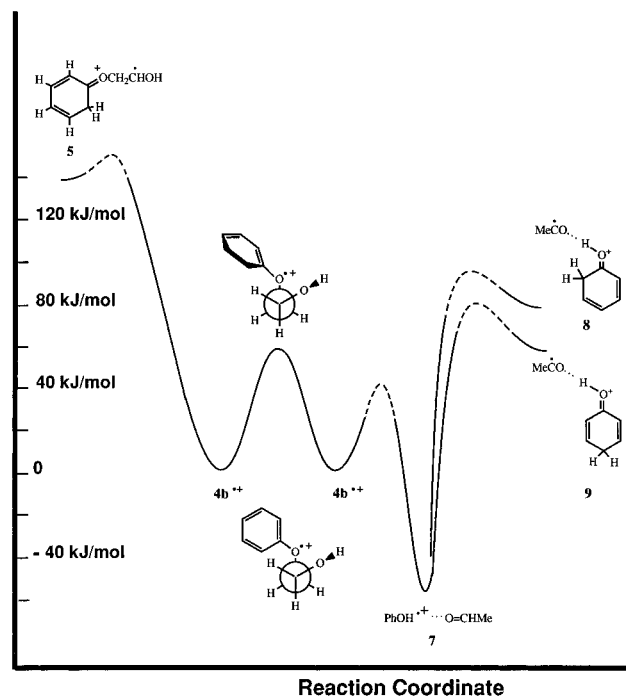
(18) Azrak, R. G.; Wilson, E. B., Jr. *J. Chem. Phys.* **1970**, *52*, 5299−5316.

Figure 3. Section of the UHF/6-31G** surface for $C_8H_{10}O_2$•+ showing the transition state for rotation of the phenyl group in **4b•+** and the plausible reactive intermediates in the decomposition that correspond to local minima: distonic ion **5** and hydrogen-bonded species **7**−**9**.

the BSSE change as well as $\Delta ZPE = -11$ kJ mol^{-1}). Endothermic hydrogen atom transfer from the aldehyde group to an *ortho*-position of the benzene ring gives **8**, which lies 25 kJ mol^{-1} above **4•+** ($\Delta BSSE$ and ΔZPE turn out to be negligible for **7** → **8**). Hydrogen atom transfer to the *para*-carbon of the ring forms a hydrogen-bonded aggregate of acetyl radical and *p*-protonated phenol, **9**, that is 20 kJ mol^{-1} more stable than **8**. We find that optimized geometries of all three of these hydrogen-bonded aggregates (**7**−**9**) possess planes of symmetry, with all the carbon and oxygen atoms in the plane. Figure 3 presents a potential energy diagram contrasting eq 3 with eq 6.

Equation 6 explains why at most one hydrogen from the chain undergoes exchange with ring hydrogens: only the aldehydic hydrogen has a low enough bond dissociation energy to transfer to the ring. The question remains, though, how **4•+** isomerizes to **7**. Since no stable hydrogen bond is present in the molecular ion, **4•+** very likely behaves as do other simple alkyl phenyl ethers, whose radical cations form ion−neutral complexes via C−O bond heterolysis in the gas phase. We presume that rearrangement of the nascent β-hydroxyethyl cation takes place concomitantly with heterolysis. We find no evidence for an SCF potential energy minimum corresponding to an ion−neutral complex. Nevertheless, it seems that one must intervene, as represented by intermediate **6** in Scheme 1, in order that the β-hydroxyethyl group does not have to rearrange simultaneously with formation of an O−H•••O hydrogen bond (which is a repulsive interaction in **4•+** but a highly attractive one in **7**).

The $\Delta H°$ (including BSSE correction and $\Delta ZPE = 3.5$ kJ mol^{-1}) for dissociating **7** at 0 K into acetaldehyde and ionized phenol is 91.5 kJ mol^{-1}. The electronic energy of **7** is 130 kJ mol^{-1} lower than that for oxirane hydrogen-bonded to ionized phenol. That energy difference is greater than the difference between neutral acetaldehyde and oxirane. Hence, the calculations imply that oxirane is a weaker hydrogen bond acceptor (by about 15 kJ mol^{-1}) than is acetaldehyde, despite the fact that oxirane is reported to have a greater proton affinity.[8]
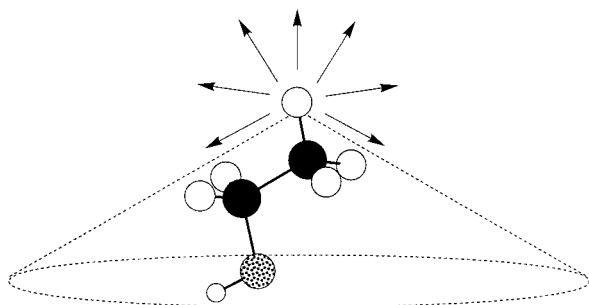
Figure 4. Schematic representation of the directions of beta-emission and ^{3}He loss that do not lead to collision of ejected particles with the remaining carbocation (represented by arrows), as compared with the volume of space (represented by the dashed 120° cone) where such collisions are possible.

Using eq 6 as a guide to Scheme 1, the following assessments can be made. Approximately 15% of metastable ionized 2-phenoxyethanol yields ionized phenol via intermediate **8** (neglecting isotope effects, half should give *m/z* 98 and half *m/z* 99 from **4**$^{•+}$-*d$_5$*), while 40% gives protonated phenol. Both pathways pass through [PhO$^•$ CH$_3$CH=OH$^+$] ion−neutral complexes. The absence of any detectable interchange of the two methylenes means that neither pathway passes through complexes containing protonated oxirane. While we can draw no conclusion regarding the remaining 45% of the metastable ions (all of which yield ionized phenol, too), it is clear that the majority of **4**$^{•+}$ heterolyzes its C−OPh bond with concomitant hydride shift, rather than bridging. This conclusion is ratified by studies of free **1** produced by tritium decay.

Free Hydroxyethyl Cations from Nuclear Decay. Beta-decay is a three-body process, which can be viewed as two successive two-body decays. For a tritium nucleus the first is the decomposition ^{3}H$^+ \rightarrow\,^3$He^{2+} + **it**$^-$, where **it**$^-$ stands for a virtual, negatively charged intermediate vector boson.[19] The second step is **it**$^- \rightarrow$ e$^-$ + $\bar{\nu}_e$, decay of the virtual particle into an electron (the beta-particle) and a neutrino.

Some (but not all) of the molecular fragments attached to a disintegrating atom become internally excited following nuclear decay. Three general mechanisms dominate: (a) an ejected particle can collide with the rest of the molecule, possibly forming a superexcited state; (b) the molecular fragment can be left behind in a deformed geometry, which relaxes to an equilibrium structure containing a high degree of vibrational excitation; (c) the molecular fragment is not left as eq 2 portrays, but rather as a multiply charged cation or as two or more smaller fragments. For the purposes of examination of eq 4, the last option can be neglected, since it should not yield either of the final neutral products (oxirane or acetaldehyde) under scrutiny. We shall argue that, while the first mechanism can produce ions that contain >2 eV internal energy, the second mechanism produces ions containing <2 eV of internal energy, which do not rearrange faster than they are quenched by reaction with gaseous base.

Consider excitation mechanism a above. The arrows in Figure 4 represent a subset of the trajectories of ejected particles with their origin at a tritium nucleus. Ethanol is drawn to scale in its most stable *s-trans* conformation, with the tritium in the position *anti*-periplanar to the hydroxyl.[20] From a vantage point at the tritium nucleus, the rest of the molecule subtends a region of space easily contained within a 120° cone, which is represented by dashed lines. The odds against the beta-particle

exiting within the cone are 3:1. If spin correlation effects are neglected (which leads to an error of a few percent, at most), the angular distribution of the ^{3}He atom is independent of the direction of the beta-particle.[19] Therefore, the odds against the ^{3}He atom exiting within the cone are also 3:1. We take the sum of the two probabilities as an upper bound for the net probability that one of the ejected particles collides with the carbocation from which it is departing. In other words, ≥50% of the carbocations are formed without being struck by an ejected particle.

Now consider excitation pathway b, vibrational excitation of carbocations that do not collide with a beta-particle or a ^{3}He atom. Of the total kinetic energy liberated by the nuclear decay (18.61 keV), an average of one-third is carried off by the neutrino (which does not interact with ordinary matter). Conservation of momentum dictates that, of the remaining kinetic energy, <0.02% is imparted to the ^{3}He nucleus. The helium atom should carry off most of this recoil as translational kinetic energy when it detaches. The tritiated carbocation may be vibrationally excited, largely as a consequence of geometrical reorganization during departure of helium, but the ion can be expected to encounter a molecule of gaseous NMe$_3$ with a rate of 2×10^{10} s^{-1}. This gives enough time for the rearrangements portrayed in eq 1 to go to completion, but not enough time for the ions to complete further unimolecular rearrangements (*e.g.*, **2a** → **3a**).

Beta-emission (the first step of eq 2) takes place on the 10^{-18} s time scale. Therefore, ^{3}He forms in association with **1a** in the geometry of the ethanol precursor. At this carbon−helium distance, r_o, the helium atom is repelled by the cationized carbon (even if it remains tetrahedral). If the nascent cation undergoes no geometrical relaxation, SCF calculations (including BSSE) give a repulsive potential of 29 kJ mol^{-1} for expelling the helium atom. If the primary sp^2 cationic center is allowed to planarize, but the OCC bond angle held at the value for ethanol, SCF calculations place the energy of the nascent cation 161 kJ mol^{-1} (including BSSE correction) above the final state. If the cation is allowed to relax completely, SCF calculations give $\Delta E = 279$ kJ mol^{-1} (including BSSE correction) for conversion of the nascent cation to the optimized geometry: **2a** with a helium atom 3.1 Å away from one of the CH$_2$ groups, with a nearly linear He−C−O angle (165°). No potential energy barrier intervenes between the nascent cation and the final geometry, which has an SCF electronic energy only 0.5 kJ below that of free **2a** plus a helium atom. It is not clear whether the local minimum corresponds to a bound geometry, since the calculated zero-point energy difference is comparable to the well depth.

If **1a** does isomerize to **2a**, the helium should be ejected as though from a slingshot, with coupling between the relaxation of the cation geometry and translation of the helium atom. It seems unlikely that all of the deformation energy is left in the carbocation when the ^{3}He departs (the second step of eq 2). The atom is accelerated to a velocity v over a distance r by the repulsive potential. If HOCH$_2$CH$_2$He$^+$ were to form in the *trans*-ethanol geometry with an initially stationary helium atom, most of the relaxation energy would be carried away by the ^{3}He as translational kinetic energy, T_{He}. In that case, the atom could be accelerated to a final velocity as high as 13.5 km s^{-1} relative to the cation. However, nuclear decay forms ^{3}He with a high initial velocity, v_o. If the maximum possible recoil energy were wholly converted into v_o of the helium atom (3.4 eV), the ^{3}He would have an initial velocity $v_o \approx 15$ km s^{-1} in the center-of-mass frame. But because the neutrino typically carries off about one-third of the decay energy, the average tritium decay imparts an initial velocity on the order of $v_o = 12$ km s^{-1}. As

(19) Commins. E. D.; Bucksbaum, P. H. *Weak Interactions of Leptons and Quarks*; Cambridge University Press: Cambridge, 1983; pp 178−190.
(20) Lovas, F. J. *J. Phys. Chem. Ref. Data* **1982**, *11*, 251−276.

v_0 and v have comparable magnitudes, the helium atom cannot be said to escape instantaneously from the carbocation.

If v_0 were very much larger than v, the helium atom would leave before the cation had time to rearrange at all. Tritiated ethanol represents a case intermediate between $v_0 = 0$ and $v_0 \gg v$. The helium atom is moving fast to begin with, so its outward motion is not completely coupled to the geometrical relaxation of the cation. However, the shape of the repulsive potential curve does not exhibit a strong dependence on the direction the helium is traveling (as long as it is not within the dashed cone drawn in Figure 4). The force exerted on the helium atom, dE/dr, should exhibit the same dependence on the C$-^3$He distance, $r_0 + r$, regardless of which of the solid arrows in Figure 4 comes closest to the direction of v_0. We derive eq 7 as a classical approximation for the relaxation energy

$$it_{He} = \int_{r_0}^{\infty} \frac{v}{v_0 + v}\left(\frac{dE}{dr}\right)(dr) \quad (7)$$

carried off as T_{He} when $v_0 \neq 0$ (in the limit where $T_{He} = \Delta E$ when $v_0 = 0$). Evaluation of the SCF potential energy curve gives a value of $T_{He} = 110$ kJ mol^{-1}. In other words, the initial velocity v_0 of the ^{3}He is fast enough that it is gone before the cation has completely relaxed, carrying off only about 40% of the relaxation energy. The partially relaxed cation structure that remains behind has a planarized primary cation center, with the oxygen approximately 2 Å away and an O$-$CH$_2-$CH$_2^+$ bond angle near 85°.

On the basis of this approximation it seems unlikely that **2a**, if formed, contains more than 2 eV (193 kJ mol^{-1}) of excess energy (unless one of the ejected particles should happen to collide with the carbocation). The reported barrier for isomerization of **2a** to **3a** (116 kJ mol^{-1})[2] is so high that RRKM calculations require ≥2 eV of internal energy for **2a** to rearrange further to **3a** as rapidly as it is quenched by collision with NMe$_3$. While this assessment neglects the partition of energy into angular momentum, we note that the geometric mean of the calculated rotational constants for the **2a** → **3a** transition state is only 3% lower than for **2a**; hence, the effective barrier height should be negligibly perturbed by overall rotation of the cation. Thus, we infer that at least one-quarter of any **2a** formed will be quenched by NMe$_3$ before it has a chance to rearrange further: less than half will be excited by collision (mechanism 1), and less than one-quarter will retain enough energy from excitation mechanism 2 to undergo rearrangement to **3a** under the experimental conditions.

Published experimental data provide a basis on which to test our model for excitation. As Figure 4 implies, nuclear decay occasionally ejects a particle that collides with the cation and excites it. An estimate can be made (from data for tritiated propane,[21] toluene,[21,22] and benzene[23]) of the fraction of carbocations produced by nuclear decay that are very highly excited. When tritium is attached to an aromatic molecule, the probability of excitation by mechanism a should be smaller than that suggested by the 120° cone in Figure 4. Decomposition of one of the tritium nuclei in [*p*-di-^{3}H]benzene in the gas phase in the presence of weak nucleophiles gives tritiated, substituted benzenes, where most of the tritium is *para* to the substituent. When the methanol is the nucleophile, 75.6% of the recovered

anisole has tritium *para* to the methoxy group, but some is *meta* (16.7%) and some is *ortho* (7.7%).[23] In liquid methanol all of the tritium is *para* to the methoxy. Similarly, halobenzenes from quenching by gaseous alkyl halides also show some transposition of tritium, albeit to a lower extent, which decreases as the pressure of nucleophile is increased. Dewar and Reynolds[24] had suggested that the gas-phase result comes from rearrangements of gaseous TC$_6$H$_4$XR$^+$, the covalent adduct of the quenching nucleophile with the *para*-tritiated phenyl cation. However, this was ruled out for X = OH by preparation of that same adduct ion (*para*-tritiated, O-protonated anisole) via an independent route in the gas phase and demonstration that it undergoes no transposition of tritium.[22] Since hydrogen rearrangement within *para*-tritiated phenyl cation has been calculated to have a barrier >170 kJ/mol (40 kcal/mol),[25] the conclusion was that about 25% of the carbocations must have been formed with a very high internal energy, large enough for hydrogen to transpose before the cation is quenched by methanol. Qualitatively this is what would be expected from the nonzero probability of collision of an ejected particle with the cation.

Our best assessment of eq 4 analyzes the products of nuclear decay as follows. For multiply tritiated ethanol, at least half the tritium is in the β-position, and no more than half of that should yield cations highly excited enough by collision with an ejected particle (excitation mechanism a) to undergo rearrangement of **2a** to **3a** prior to quenching. No more than half of the remainder should contain enough internal energy from deformation to rearrange prior to being quenched. With an observed acetaldehyde:oxirane ratio ≥ 40:1, we therefore conclude that the branching ratio for eq 1 following nuclear decay of TCH$_2$CH$_2$OH is ii:i ≥ 5:1. Ethanol consists of rapidly interconverting conformers at room temperature,[20] but the most abundant has *s-trans* geometry with a plane of symmetry (illustrated in Figure 4). Approximately 30% of the decaying tritium atoms vicinal to oxygen will be *anti*-periplanar to the hydroxyl in the *s-trans* conformation. We therefore conclude that hydride shift (pathway ii) predominates over bridging (pathway i in eq 1), even starting from a geometry (tritium *anti*-periplanar to oxygen) for which ab initio geometry optimization predicts smooth, barrier-free conversion to a bridged ion. Whether this discrepancy between computation and experiment is purely an energetic effect remains to be investigated.

Conclusions

This study draws parallels between two types of experiments using hydrogen isotope labeling to investigate rearrangements of ion **1**, a nascent species that is not expected to be stable. Heterolyis of the C$-$OPh bond of ionized 2-phenoxyethanol is probed in the mass spectrometer using deuterium labeling. Nuclear decay of [^{3}H]methyl groups in tritiated ethanol yields neutral products, in which acetaldehyde greatly predominates over oxirane. Our analysis of the data leads to the following conclusions.

(1) Metastable ionized 2-phenoxyethanol decomposes via complexes, most (if not all) of which are of the form [PhO$^\bullet$ CH$_3$-CH=OH$^+$].

(2) The majority of these complexes subsequently pass through hydrogen-bonded intermediates, whose intervention is confirmed by UHF calculations that show their stability.

(21) Wexler, S.; Anderson, G. R.; Singer, L. A. *J. Chem. Phys.* **1960**, *32*, 417−427.

(22) Cacace, F.; Cipollini, R.; Giacomello, P. *J. Phys. Chem.* **1982**, *86*, 2062−2065.

(23) Angelini, G.; Fornarini, S.; Speranza. M. *J. Am. Chem. Soc.* **1982**, *104*, 4773−4780. (b) Speranza, M.; Keheyan, Y.; Angelini, G. *J. Am. Chem. Soc.* **1983**, *105*, 6377−6380.

(24) Dewar, M. J. S.; Reynolds, C. H. *J. Am. Chem. Soc.* **1982**, *104*, 3244−3246.

(25) Schleyer, P. v. R.; Kos, A. J.; Raghavachari, K. *J. Chem. Soc., Chem. Commun.* **1983**, 1296−1298.

(3) Hydride shift predominates in C−OPh heterolyses when the neighboring group is hydroxy, in contrast to what can be inferred from published data on analogous ions containing a neighboring amino group[4] or halogen.[5,6,14]

(4) Nuclear decay of tritium bound to carbon forms cations, which may be excited during their formation in two ways: (a) by collision of an ejected particle with the molecular fragment (which can produce superexcited ions with energies often >2 eV) or (b) by relaxation of an initially deformed structure (which, for the most part, produces ions with internal energies <2 eV).

(5) Evaluation of the possible pathways to tritiated acetaldehyde from TCH_2CH_2OH leads to an experimental ratio of hydride shift to bridging of ≥5:1, contrary to expectations based on ab initio calculations, which predict oxygen bridging.

Mass spectrometry and tritium decay lead independently to the same conclusion. This outcome is surprising in light of the extent of bridging by vicinal hydroxy reported for gaseous ions derived from 3-hydroxy-2-butyl systems.[7] No obvious reason presents itself as to why hydride shift prevails in the less highly substituted case, **1a**. In any event, nuclear decay of tritiated

ethanol provides a source of gaseous **3a**, whose bimolecular reactions with nucleophiles are under current investigation.

Supporting Information Available: Tables giving the UHF-optimized Cartestian coordinates for ions **4b**[•+], **7**, and **8** in Table 1 and a figure showing the MIKE spectra of O-deuterated compounds in Table 2 (2 pages). See any current masthead page for ordering and Internet access instructions.

JA964475V